Structural Aspects of the Coordination of Triethylphosphinegold(I) to 2-Thiouracil: A Comparison between Theory and Experiment

Gerarda M. Stewart, Edward R. T. Tiekink, and Mark A. Buntine*

Department of Chemistry, The University of Adelaide, Australia 5005

Received: January 16, 1997; In Final Form: May 7, 1997[⊗]

The interaction of the thionucleobase 2-thiouracil with the triethylphosphinegold(I) cation has been examined employing ab initio molecular orbital theory. Deprotonation of 2-thiouracil (2-TUH) and subsequent association with $[Et_3PAu]^+$ leads to the formation of $[Et_3PAu(2\text{-}TU\_H)]$; a comparison of calculated and experimental geometric parameters reveals a high degree of agreement. The interaction of two $[Et_3PAu]^+$ cations with twice deprotonated 2-TUH indicates that the most stable dinuclear structure is one where coordination occurs via the sulfur and one of the nitrogen atoms leading to almost linear P−Au−S and P−Au−N arrangements, respectively.

1. Introduction

The use of gold in medicine is well documented, with gold compounds being used clinically in the treatment of rheumatoid arthritis, i.e., crysotherapy.[1] Toxicity and other side effects associated with crysotherapy, and indeed heavy-metal therapy in general, motivate research into alternative potent metal/ligand combinations. Interest in the chemistry of thionucleobases and their triorganophosphinegold(I) complexes thus arises as a result of their reported biological activity. For example, the triphenylphosphinegold(I) 6-mercaptopurinate complex **1** displays both in vivo antiarthritic activity[2] and in vitro/in vivo cytotoxicity.[3] Analogous complexes containing the thionucleobase 2-thiouracil (**2**, 2-TUH, showing numbering scheme) also display promising activity,[4] and this system forms the basis of the present study.

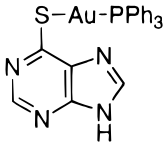

1

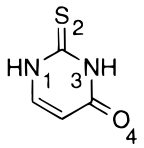

2

Generally, antiarthritic gold complexes fall into two classes. The first of these classes is exemplified by myocrisin (**3**), which is (i) charged and (ii) polymeric. By contrast, auranofin (**4**) is neutral and monomeric.

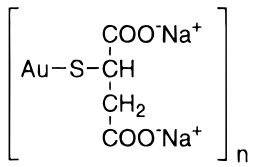

3

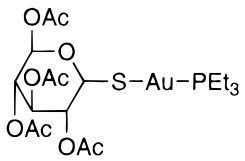

4

The different chemical forms of these complexes dictates that they are administered differently, with the former being injected owing to its water solubility and the latter, lipid soluble species, ingested orally. A feature of the gold drugs used clinically is the presence of linear, or near to linear, gold atom geometries. It is thought that this arrangement facilitates ligand exchange in biological media through a three-coordinate intermediate and hence may be important for biological potency.[5] A current focus of research in this area is aimed at forming neutral, lipophilic gold-rich species in order to obtain compounds with characteristics intermediate to the polymeric and monomeric species cited above but retaining the possibility of oral administration.

In this contribution, the feasibility of forming such gold-rich species is explored, as determined by ab initio calculations, using 2-TUH as the template. Thus, the ab initio-determined structures of 2-TUH, $[2\text{-}TU\_H]^-$, $[Et_3PAu(2\text{-}TU\_H)]$, and $[Et_3PAu(2\text{-}TU\_2H)AuPEt_3]$ are described and compared to their X-ray crystal structures when possible. In particular, we are interested in exploring whether molecular orbital theory can be used as a means of predicting the likely biological activity of gold(I)-containing compounds based upon their structural characteristics.

2. Computational Details

All geometry optimizations were performed using the GAUSSIAN 94 suite of programs[6] run on Silicon Graphics Indigo^{2}xZ Workstation and Silicon Graphics Power Challenge computers. All calculations were performed at the Hartree−Fock SCF level of theory. Unless specified otherwise, calculations were performed using the LanL2DZ basis set.[6] The LanL2DZ basis set employs the Dunning/Huzinaga double-ζ descriptor[7] for all first-row elements and replaces the core electrons of phosphorus (up to 2*p*), sulfur (up to 2*p*) and gold (up to 4*f*) with the effective core potentials (ECPs) of Hay and Wadt.[8,9]

3. Results and Discussion

3.1. 2-Thiouracil. Optimized geometries for 2-TUH were determined at the Hartree−Fock level of theory. Basis sets used include 3-21G*, 6-31++G**, 6-311++G**, and LanL2DZ; selected geometric parameters are collected in Table 1. An optimized geometry of 2-TUH has been reported previously employing GAUSSIAN 88 with the 3-21G* basis set,[10] and the results reported in Table 1 are in agreement with this earlier study. The LanL2DZ basis set was chosen for further calculations to ultimately enable the study of the interaction between $[2\text{-}TU\_H]^-$ and $[Et_3PAu]^+$, i.e., for structures incorporating post-second-period elements, particularly gold. Confidence in the geometric parameters determined with the LanL2DZ basis set is found in the close agreement between these results and those obtained using the Pople basis sets (Table 1). Importantly, the results show that there is little, if any, significant influence on

[⊗] Abstract published in *Advance ACS Abstracts,* June 15, 1997.

S1089-5639(97)00223-5 CCC: $14.00

TABLE 1: Geometric Parameters (Å, deg) for 2-Thiouracil (2) Obtained from the 3-21G*, 6-31++G, 6-311++G**, and LanL2DZ Basis Sets and the Crystal Structure Analysis**

parameter	3-21G*[a]	3-21G*[b]	6-31++G**[b]	6-311++G**[b]	LanL2DZ[b]	X-ray[c]
S(2)−C(2)	1.661	1.662	1.664	1.661	1.716	1.683(3)
O(4)−C(4)	1.210	1.209	1.193	1.187	1.223	1.227(4)
N(1)−C(2)	1.361	1.355	1.353	1.353	1.363	1.338(4)
N(1)−C(6)	1.380	1.361	1.374	1.374	1.387	1.373(4)
N(1)−H(1)	0.999	0.999	0.995	0.994	0.995	0.90(5)
N(3)−C(2)	1.355	1.404	1.351	1.353	1.361	1.357(4)
N(3)−C(4)	1.404	1.455	1.397	1.398	1.405	1.389(4)
N(3)−H(3)	1.002	1.002	0.998	0.998	0.999	0.90(4)
C(4)−C(5)	1.455	1.326	1.460	1.460	1.460	1.432(5)
C(5)−C(6)	1.326	1.380	1.331	1.328	1.341	1.338(5)
C(5)−H(5)	1.066	1.066	1.070	1.070	1.067	0.84(4)
C(6)−H(6)	1.069	1.069	1.073	1.073	1.069	0.94(4)
S(2)−C(2)−N(1)	122.3	122.3	122.3	122.3	122.2	122.2(2)
S(2)−C(2)−N(3)	116.4	123.5	123.3	123.3	123.2	121.8(2)
O(4)−C(4)−N(3)	120.3	120.3	120.1	120.2	120.0	119.2(3)
O(4)−C(4)−C(5)	118.5	126.3	126.0	126.0	125.7	125.4(3)
C(2)−N(1)−C(6)	123.2	123.2	123.5	123.4	123.3	122.9(3)
N(1)−C(2)−N(3)	114.2	114.2	114.4	114.4	114.6	116.0(3)
N(1)−C(6)−C(5)	121.8	121.8	121.9	122.0	121.6	121.2(3)
N(3)−C(4)−C(5)	113.4	113.4	113.9	113.8	114.3	115.4(3)
C(2)−N(3)−C(4)	127.8	127.8	127.5	127.6	127.1	125.2(3)
C(4)−C(5)−C(6)	119.7	119.7	118.8	118.9	119.0	119.2(3)

[a] Reference 10. [b] This work. [c] Reference 11.

geometric parameters by the inclusion of polarization and/or diffuse functions in the basis set. Moreover, the reproducibility in geometric parameters with different basis sets gives us faith that the use of ECPs to describe the electronic structure of sulfur (and later on, phosphorus and gold) is a valid approximation. A comparison of the optimized structure of 2-TUH at any basis set with the crystallographically determined structure[11] shows that there is very good agreement. The reported crystal structure shows that 2-TUH exists in the thione−lactam form as indicated in **2**, and the theoretical results agree with this structural assignment. Minor differences between the structures are attributed to the different phases (gaseous versus solid state) used for calculation and experiment.

3.3. [Et$_3$PAu(2-TU_H)]. An ab initio investigation into the structure and energetics of various metal cations interacting with guanine and adenine has very recently been reported by Hobza and co-workers, who are interested in elucidating the role of metal ions in the biophysics of DNA.[12] In the cited study the interactions of selected cations (ranging from Li^+ to Hg^{2+}, and including Au^+) with the isolated bases are reported. This work is of particular relevance to the study reported here. For the smaller ions studied (Na^+, K^+, Mg^{2+}, and Ca^{2+}), Hobza and co-workers employed both all-electron and pseudopotentials to describe the electronic structure of the metal ion. An important result of this work is that geometries reported using both the all-electron and pseudopotential treatments yielded very good agreement. Hobza and co-workers went on to use the pseudopotentials for heavier cations with confidence.

The elegant work from Hobza's laboratory highlights an exciting new theoretical approach to probing the dynamics of metal ion−nucleobase interactions. However, to be sure that conclusions drawn from molecular structures determined using ECP (i.e., pseudopotential)-based molecular orbital calculations have sound predictive reliability, some comparison to experimental results is essential. We now go on to compare the reported crystal structure of [Et$_3$PAu(2-TU_H)][4] with that determined theoretically.

The crystallographically determined structure of [Et$_3$PAu(2-TU_H)][4] features a linear P−Au−S arrangement as found in auranofin (**4**). To prepare this compound, deprotonation of 2-TUH must occur, and coordination of [Et$_3$PAu]$^+$ to sulfur eventuate. Calculations using the LanL2DZ basis set show that deprotonation at the N(1) site is 59 kJ mol^{-1} more favorable than at the N(3) atom. This result indicates that structure **2a** is preferred over **2b**; the use of the 6-31++G** and 6-311++G** basis sets leads to the same conclusion (ΔE = 53 and 52 kJ mol^{-1}, respectively). Resonance of **2a** with **2c** (and the **2b** equivalent, **2d**) leads to a thiolate ligand which may coordinate with [Et$_3$PAu]$^+$.

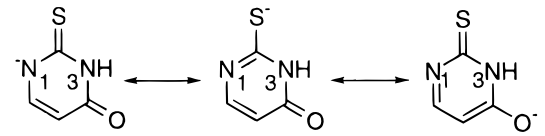

2a **2c** **2e**

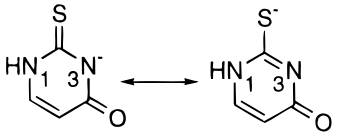

2b **2d**

A simple understanding of why deprotonation of **2** (yielding **2a**) at site N(1) results in the formation of a Au−S bond, rather than a Au−N(1) bond, upon gold(I) complexation can be found from an analysis of the changes in Mulliken population following deprotonation. The Mulliken charge distributions for 2-TUH (**2**) and [2-TU_H]$^-$ (**2a**) are given in Table 2, along with the change in population for each atom following deprotonation. A positive value in the changes given in Table 2 represents an increase in the Mulliken population for that atom. Clearly, the site of negative charge following deprotonation is at the sulfur atom, indicating that structure **2c** is preferred over **2a**. With the negative charge largely localized on the sulfur atom, coordination of [Et$_3$PAu]$^+$ to S(2) is expected.

Mulliken population analysis, like all atomic charge assignment schemes, is an arbitrary method for assigning atomic

TABLE 2: Changes in Mulliken Population[a] between 2-TUH (2) and [2-TU_H]$^-$ (2a)

atom	2	2a	$\Delta_{population}$
S(2)	−0.051	−0.363	−0.312
O(4)	−0.398	−0.485	−0.087
N(1)	−0.513	−0.233	0.280
N(3)	−0.550	−0.618	−0.068
C(2)	−0.094	−0.125	−0.031
C(4)	0.468	0.461	−0.007
C(5)	−0.279	−0.366	−0.087
C(6)	0.036	−0.073	−0.109
H(1)	0.427		
H(3)	0.445	0.406	−0.039
H(5)	0.262	0.209	−0.053
H(6)	0.247	0.187	−0.060

[a] A positive value represents an increase in the Mulliken population.

TABLE 3: Changes in Natural Population[a] between 2-TUH (2) and [2-TU_H]$^-$ (2a)

atom	2	2a	$\Delta_{population}$
S(2)	−0.281	−0.476	−0.195
O(4)	−0.684	−0.819	−0.136
N(1)	−0.670	−0.715	−0.016
N(3)	−0.740	−0.750	−0.011
C(2)	0.439	0.438	−0.001
C(4)	0.807	0.799	−0.008
C(5)	−0.380	−0.478	−0.098
C(6)	0.139	0.160	0.021
H(1)	0.458		
H(3)	0.467	0.441	−0.025
H(5)	0.248	0.212	−0.036
H(6)	0.227	0.189	−0.038

[a] A positive value represents an increase in the natural population.

charges. Generally, *changes* in Mulliken population provide a reasonable estimation of changes in electron density within closely related molecules. Mulliken population analysis assigns atomic charges by dividing molecular orbital overlap evenly between each pair of atoms involved in a chemical bond. To identify any artifacts in the Mulliken population analysis, a natural population analysis[13] was also performed. The natural charges for each atom in 2-TUH (**2**) and [2-TU_H]$^-$ (**2a**) are given in Table 3, along with the changes in natural charge upon deprotonation. Again we see a strong localization of negative charge on the sulfur atom rather than at the N(1) site of deprotonation. The natural charge analysis also shows that some negative charge migrates to the oxygen atom following deprotonation, consistent with structure **2e**.

The structure of [2-TU_H]$^-$ has been experimentally determined as the counterion for the gold complex $[Au(Ph_2PCH_2CH_2PPh_2)_2]^+$.[4] The structure crystallizes with a neutral [2-TUH] molecule in the lattice so that the overall composition is $[Au(Ph_2PCH_2CH_2PPh_2)_2]$[(2-TUH)(2-TU_H)]. Deprotonation of [2-TU_H] occurs at N(1), and an analysis of the derived interatomic parameters suggests that **2c** is the dominant resonance contributor. However, there is also some evidence for a contribution to the overall structure by **2e**. That is, there is experimental evidence for some formal negative charge residing on the O(4) atom.[4] Selected interatomic parameters, determined experimentally and by calculation, for [2-TU_H]$^-$ are listed in Table 4. These show that while there is some evidence for elongation of the C(4)−O(4) bond in the calculated structure, the calculated parameters match more closely those expected for **2c**. If **2e** was dominant, we would anticipate significant elongation of the C(4)−O(4) bond. Minor differences between the experimental and calculated geometric parameters probably arise as a result of the significant hydrogen-bonding interactions between the neutral and deprotonated molecules in the crystal lattice.[4]

TABLE 4: Geometric Parameters (Å, deg) for [2-TU_H]$^-$ Obtained from the Crystal Structure Determination[4] and the LanL2DZ Basis Set

parameter	X-ray	LanL2DZ
S(2)−C(2)	1.693(7)	1.758
O(4)−C(4)	1.235(8)	1.252
N(1)−C(2)	1.361(8)	1.334
N(1)−C(6)	1.34(1)	1.360
N(3)−C(2)	1.351(8)	1.391
N(3)−C(4)	1.369(9)	1.387
C(4)−C(5)	1.41(1)	1.438
C(5)−C(6)	1.38(1)	1.370
S(2)−C(2)−N(1)	121.2(5)	124.9
S(2)−C(2)−N(3)	120.2(5)	117.0
N(1)−C(2)−N(3)	118.6(6)	118.1
C(2)−N(1)−C(6)	117.7(6)	118.2
C(2)−N(3)−C(4)	126.2(5)	126.6
O(4)−C(4)−N(3)	120.7(6)	120.1
O(4)−C(4)−C(5)	125.1(7)	126.6
N(3)−C(4)−C(5)	114.2(6)	113.3

TABLE 5: Geometric Parameters (Å, deg) for [Et_3PAu(2-TU_H)] (5a) Obtained from the Crystal Structure Determination[4] and the LanL2DZ Basis Set

parameter	X-ray	LanL2DZ
Au−P(1)	2.248(2)	2.437
Au−S(2)	2.310(2)	2.462
S(2)−C(2)	1.719(9)	1.792
O(4)−C(4)	1.24(1)	1.235
N(1)−C(2)	1.31(1)	1.307
N(1)−C(6)	1.37(1)	1.383
N(3)−C(2)	1.349(9)	1.371
N(3)−C(4)	1.38(1)	1.398
C(4)−C(5)	1.40(1)	1.450
C(5)−C(6)	1.35(2)	1.355
P(1)−Au−S(2)	176.9(1)	179.7
Au−S(2)−C(2)	101.4(3)	99.4
Au−P(1)−C(11)	121.1(3)	114.8
Au−P(1)−C(21)	111.3(3)	112.1
Au−P(1)−C(31)	115.4(3)	112.9
S(2)−C(2)−N(1)	122.9(6)	122.9
S(2)−C(2)−N(3)	115.8(6)	116.0
N(1)−C(2)−N(3)	121.3(8)	121.2
C(2)−N(3)−C(4)	125.0(7)	124.6
C(2)−N(1)−C(6)	116.8(8)	117.6
Au−S(2)−C(2)−N(1)	3.7(4)	0.2
Au−S(2)−C(2)−N(3)	−175.6(3)	−179.8

Calculations describing the coordination of $[Et_3PAu]^+$ to thiolates **2c** and **2d** indicate that structure **5a** is the most energetically stable by 23 kJ mol^{-1}, over **5b**. This result is in accord with the X-ray crystal structure of this compound.[4] Selected interatomic parameters for the observed and calculated structures are listed in Table 5, and a view of the optimized geometry is represented in Figure 1. A comparison of the calculated and experimental parameters shows that except for the expected elongation of the bond distances, in particular for those involving the gold atom, and minor conformational changes in the phosphorus-bound ethyl groups, there is close agreement between observed and calculated structures. It is important to note that the linearity of the P−Au−S arrangement is reproduced in the calculated structure and that a weak Au···N(1) interaction of 3.113(2) Å observed in the crystal structure is retained in the calculated structure, where the Au···N(1) separation is 3.192 Å.

As there is experimental evidence for structure **2e**,[4] i.e., with residual charge on the O(4) atom, its interaction with $[Et_3PAu]^+$ was also investigated. Calculations show that structure **5c** is

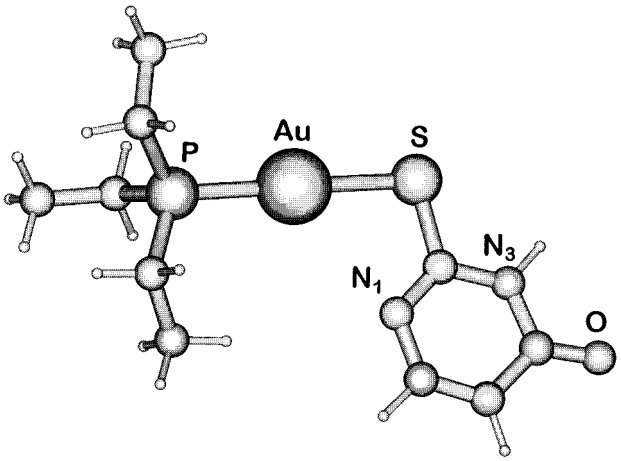

Figure 1. Optimized geometry for [Et_3PAu(2-TU_H)] (**5a**).

energetically less favorable than coordination to produce structure **5a** by 77 kJ mol^{-1}. Structure **5d** is 79 kJ mol^{-1} less stable than **5a**. Experimentally, structures **5c** and **5d** are not observed.

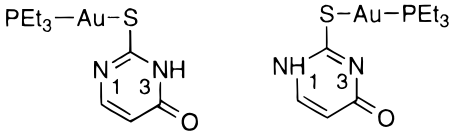

5a

5b

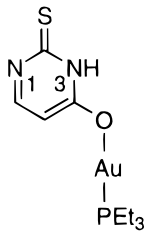

5c

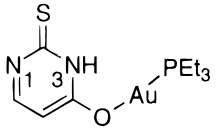

5d

Analysis of the molecular orbital coefficients of structure **5a** shows that there is considerable mixing of the valence electrons of the gold atom with *both* S(2) and N(1). The strongest interaction of the metal atom with the thionucleobase is via the π-bonding network within the six-membered ring. Considerable delocalization of the π-electron system over both the gold atom and the ring accounts for the observation of the gold atom being coplanar with the heterocyclic ring (see Table 5).

3.3. [Et_3PAu(2-TU_2H)AuPEt$_3$]. Having established the optimized structure of [Et_3PAu(2-TU_H)], this compound was deprotonated at N(3) and its interaction with a second [Et_3PAu]$^+$ moiety investigated. This is in keeping with the aim of this study, which has as its focus the formation of neutral, lipophilic species suitable for oral administration. This leads to the neutral, gold-rich species [Et_3PAu(2-TU_2H)AuPEt$_3$]. Deprotonation of **5a** at N(3) yields structures **6a** and after resonance, **6b**, suggesting that N(3) and O(4) are possible sites for [Et_3PAu]$^+$ coordination, respectively.

The geometrically optimized structures for the interaction of two [Et_3PAu]$^+$ cations with [2-TU_2H]$^{2-}$ are shown as structures **7a**, **7b** (to allow for possible rotation about the C−S bond in **5a** and subsequent coordination of [Et_3PAu]$^+$ at the N(1) atom), and **7c** (featuring a Au−O interaction rather than a Au−N interaction). Structure **7a** is energetically preferred over **7b** by 19 kJ mol^{-1}. This result is consistent with our earlier conclusion that initial deprotonation at N(1) is the energetically preferred process. Structure **7c**, however, represents the stable molecular geometry if coordination at O(4) is preferred. Interestingly, **7c** is less stable than **7a** by only 5.2 kJ mol^{-1}.

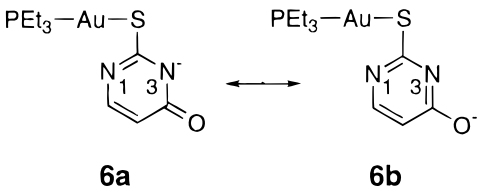

6a **6b**

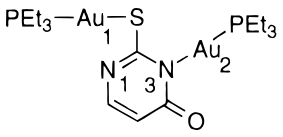

7a

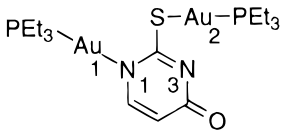

7b

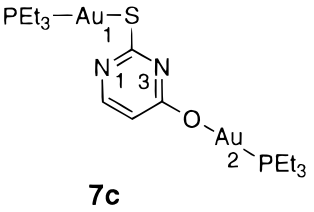

7c

The optimized structure of **7a** shows that the basic framework of **5a** is maintained and that the second [Et_3PAu]$^+$ cation is attached via the N(3) atom. Selected geometric parameters for **7a** are collected in Table 6, and the optimized geometry is shown in Figure 2. For the sake of comparison, selected geometric parameters for **7c** are collected in Table 7. Analysis of the molecular orbital coefficients of **7a** shows a strong mixing of both the Au(1) and Au(2) valence electrons with the π-cloud of the thiouracil ring. This strong mixing of the delocalized MO system accounts for the coplanarity of the Au(1) and Au(2) atoms with the ring plane (see Table 6). This latter result is consistent with the planarity observed in structure **5a**.

A crystal structure of [Et_3PAu(2-TU_2H)AuPEt$_3$] is not available for comparison with the theoretically predicted geometries. However, an examination of the relevant geometric parameters of **7a** and **7c** shows good agreement with those calculated for **5a**. The linearity about both of the Au(1) and Au(2) atoms has been retained in **7a**, and the Au(2)−N(3) distance of 2.088 Å is comparable to the Au−N distance of 2.057(5) Å found in the structure of [Et_3PAu(adeninato-*N*(9)].[14] Whereas the intramolecular Au(2)···S(2) separation of 3.377 Å is not considered significant, the Au(1)···N(1) contact of 3.068 Å is similar to that found in the crystal structure of **5a**. Structure **7c** also exhibits linearity about each of the gold atoms. Because **7c** is predicted to be only 5.2 kJ mol^{-1} energetically less stable than the lowest energy isomer, **7a**, it is possible that this species could exist in equilibrium with **7a**. In any case, from the putative conclusion that linearity about gold atoms leads to effective biological activity, we would expect both **7a** and **7c** to exhibit enhanced biological activity compared to **5a**.

The feasibility of forming dinuclear gold compounds such as **7a** is supported by the reported preparation of related dinuclear compounds with 6-thioguanine and 2,6-dithioxanthine as the templates;[15] no biological results have been reported for these compounds. Although not involving a thionucleobase, it

TABLE 6: Geometric Parameters (Å, deg) for [Et_3PAu(2-TU_2H)$AuPEt_3$] (7a) Obtained from the LanL2DZ Basis Set

parameter	
Au(1)−P(1)	2.441
Au(1)−S(2)	2.451
Au(2)−N(3)	2.105
Au(2)−P(2)	2.417
S(2)−C(2)	1.810
O(4)−C(4)	1.251
N(1)−C(2)	1.325
N(1)−C(6)	1.371
N(3)−C(2)	1.353
N(3)−C(4)	1.393
C(4)−C(5)	1.446
C(5)−C(6)	1.359
C(5)−H(5)	1.069
C(6)−H(6)	1.072
P(1)−Au(1)−S(2)	178.5
P(2)−Au(2)−N(3)	178.3
Au(1)−S(2)−C(2)	98.1
Au(2)−N(3)−C(2)	124.8
Au(2)−N(3)−C(4)	114.1
S(2)−C(2)−N(1)	118.9
S(2)−C(2)−N(3)	117.0
C(2)−N(1)−C(6)	116.7
C(2)−N(3)−C(4)	121.1
O(4)−C(4)−C(5)	124.3
N(1)−C(2)−N(3)	124.1
N(3)−C(4)−C(5)	115.8
C(4)−C(5)−C(6)	118.6
N(1)−C(6)−C(5)	123.8
Au(1)−S(2)-C(2)−N(1)	0.3
Au(1)−S(2)-C(2)−N(3)	−179.7
Au(2)−N(3)-C(2)−S(2)	−0.1
Au(2)−N(3)-C(2)−N(1)	179.9

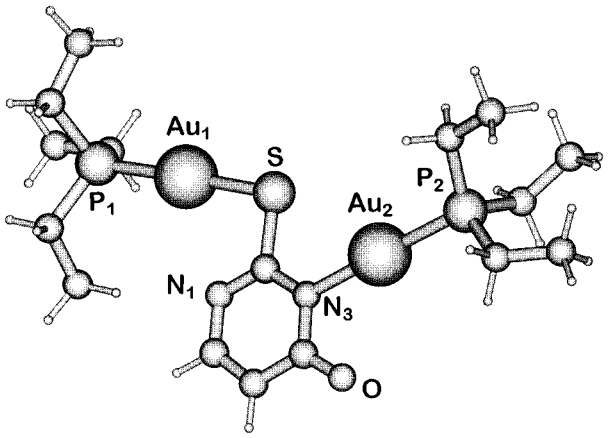

Figure 2. Optimized geometry for [Et_3PAu(2-TU_2H)$AuPEt_3$] (**7a**).

is relevant to cite the X-ray determined structures of two compounds containing the pyridine-2-thiolate anion, each of which feature effectively linear gold atom geometries. The 1:1 complex [Ph_3PAu(2-pyS)] shows a structure similar to that represented in **5a**.[16] The [2-pyS]$^-$ anion can also bridge two gold atoms via the sulfur and nitrogen atoms as shown in the structure of {[$Ph_2P(CH_2Au)_2$](2-pyS)}, in which the gold-bound phosphine ligands have been substituted for carbons in this organometallic compound.[17]

4. Conclusions

This study has shown that ab initio molecular orbital calculations employing ECPs is eminently suitable for performing geometry optimizations on biologically significant compounds containing gold. The feasibility of preparing lipophilic gold rich species, constructed about thionucleobases (specifically 2-thiouracil) has been explored, and the study shows that there are no steric obstacles to their formation. Our calculations demonstrate that deprotonation of 2-TUH is favored at N(1), and coordination of one $[Et_3PAu]^+$ cation occurs preferentially at S(2), yielding structure **5a**. This result is in accord with crystallographic data.[4] A second $[Et_3PAu]^+$ entity preferentially coordinates at the N(3) atom leading to **7a**, which features essentially linear P−Au−S and P−Au−N arrangements. Alternatively, a second $[Et_3PAu]^+$ may coordinate at the O(4) site, resulting in structure **7c**. This latter geometry has been shown to be only 5.2 kJ mol^{-1} less stable than **7a**. Importantly, however, it retains linearity about both gold atom centers. Linearity about the gold atoms is thought to play an important role in the molecules' biological activity[5] and such arrangements have been demonstrated in [Et_3PAu(2-TU_H)] and [Et_3PAu(2-TU_2H)$AuPEt_3$]. This work represents an important step toward predicting the potential of compounds to exhibit biological potency.

TABLE 7: Geometric Parameters (Å, deg) for [Et_3PAu(2-TU_2H)$AuPEt_3$] (7c) Obtained from the LanL2DZ Basis Set

parameter	
Au(1)−P(1)	2.444
Au(1)−S(2)	2.441
Au(2)−P(2)	2.400
Au(2)−O(4)	2.086
S(2)−C(2)	1.807
O(4)−C(4)	1.307
N(1)−C(2)	1.343
N(1)−C(6)	1.352
N(3)−C(2)	1.337
N(3)−C(4)	1.349
C(4)−C(5)	1.418
C(5)−C(6)	1.377
C(5)−H(5)	1.068
C(6)−H(6)	1.072
P(1)−Au(1)−S(2)	178.7
P(2)−Au(2)−O(4)	177.4
Au(1)−S(2)−C(2)	99.1
Au(2)−O(4)−C(4)	118.2
S(2)−C(2)−N(1)	119.3
S(2)−C(2)−N(3)	116.7
C(2)−N(1)−C(6)	116.6
C(2)−N(3)−C(4)	120.0
O(4)−C(4)−C(5)	121.9
N(1)−C(2)−N(3)	124.0
N(3)−C(4)−C(5)	119.3
C(4)−C(5)−C(6)	116.7
N(1)−C(6)−C(5)	0.4
Au(1)−S(2)−C(2)−N(1)	0.4
Au(1)−S(2)−C(2)−N(3)	−179.6
Au(2)−O(4)−C(4)−N(3)	−0.1
Au(2)−O(4)−C(4)−C(5)	180.0

Acknowledgment. This work was supported by the University of Adelaide. Computing resources provided by the South Australian Centre for Parallel Computing (SACPC) are gratefully acknowledged.

References and Notes

(1) Parish, R. V. *Interdisciplinary Sci. Rev.* **1992**, *17*, 15. Sadler, P. J.; Sue, R. E. *Metal-Based Drugs* **1994**, *1*, 107. Tiekink, E. R. T.; Whitehouse, M. W. In Berthon, G., Ed. *Handbook of Metal−Ligand Interactions in Biological Fluids*; Marcel Dekker Inc.: New York, 1994; Vol. 2, p 71.

(2) Cookson, P. D.; Tiekink, E. R. T.; Whitehouse, M. W. *Aust. J. Chem.* **1994**, *47*, 577.

(3) Tiekink, E. R. T.; Cookson, P. D.; Linahan, B. M.; Webster, L. K. *Metal-Based Drugs* **1994**, *1*, 299. Webster, L. K.; Rainone, S.; Horn, E.; Tiekink, E. R. T. *Metal-Based Drugs* **1996**, *3*, 63.

(4) Harker, C. S. W.; Tiekink, E. R. T.; Whitehouse, M. W. *Inorg. Chim. Acta* **1991**, *181*, 23.

(5) Shaw, C. F. In Fricker, S. P., Ed., *Metal Compounds in Cancer Therapy*; Chapman and Hall: London, 1994; p 46.
(6) Gaussian 94, Revision D.3; Frisch, M. J.; Trucks, G. W.; Schlegel, H. B.; Gill, P. M. W.; Johnson, B. G.; Robb, M. A.; Cheeseman, J. R.; Keith, T.; Petersson, G. A.; Montgomery, J. A.; Raghavachari, K.; Al-Laham, M. A.; Zakrzewski, V. G.; Ortiz, J. V.; Foresman, J. B.; Cioslowski, J.; Stefanov, B. B.; Nanayakkara, A.; Challacombe, M.; Peng, C. Y.; Ayala, P. Y.; Chen, W.; Wong, M. W.; Andres, J. L.; Replogle, E. S.; Gomperts, R.; Martin, R. L.; Fox, D. J.; Binkley, J. S.; Defrees, D. J.; Baker, J.; Stewart, J. P.; Head-Gordon, M.; Gonzalez, C.; Pople, J. A. Gaussian Inc.: Pittsburgh, PA, 1995.
(7) Dunning Jr.; T. H.; Hay, P. J. In *Modern Theoretical Chemistry*; Schaefer III, H. F., Ed.; Plenum: New York, 1976, p 1.
(8) Wadt , W. R.; Hay, P. J. *J. Chem. Phys.* **1985**, *82*, 284.
(9) Hay, P. J.; Wadt, W. R. *J. Chem. Phys.* **1985**, *82*, 299.
(10) Les, A.; Adamowicz, L. *J. Am. Chem. Soc.* **1990**, *112*, 1504.
(11) Tiekink, E. R. T. *Z. Kristallogr.* **1989**, *187*, 79.
(12) Burda, J. V.; Sponer, J.; Hobza, P. *J. Phys. Chem.* **1996**, *100*, 7250.
(13) Glendening, E. D.; Reed, A. E.; Carpenter, J. E.; Weinhold, F. NBO, Version 3.1.
(14) Tiekink, E. R. T.; Kurucsev, T.; Hoskins, B. F. *J. Cryst. Spectrosc. Res.* **1989**, *19*, 823.
(15) Stocco, G.; Gattuso, F.; Isab, A. A.; Shaw, C. F. *Inorg. Chim. Acta* **1993**, 209, 129.
(16) Cookson, P. D.; Tiekink, E. R. T. *J. Chem. Soc., Dalton Trans* **1993**, 259.
(17) Bardaji, M.; Connelly, N. G.; Gimeno, M. C.; Jones, P. G.; Laguna, A.; Laguna, M. *J. Chem. Soc., Dalton Trans* **1995**, 2245.